

# Second Order Statistical Behavior of LLL and BKZ

Yang Yu<sup>1</sup> and Léo Ducas<sup>2</sup>

<sup>1</sup> Department of Computer Science and Technology, Tsinghua University, Beijing, China

[y-y13@mails.tsinghua.edu.cn](mailto:y-y13@mails.tsinghua.edu.cn)

<sup>2</sup> Cryptology Group, CWI, Amsterdam, The Netherlands  
[ducas@cwi.nl](mailto:ducas@cwi.nl)

**Abstract.** The LLL algorithm (from Lenstra, Lenstra and Lovász) and its generalization BKZ (from Schnorr and Euchner) are widely used in cryptanalysis, especially for lattice-based cryptography. Precisely understanding their behavior is crucial for deriving appropriate key-size for cryptographic schemes subject to lattice-reduction attacks. Current models, *e.g.* the Geometric Series Assumption and Chen-Nguyen’s BKZ-simulator, have provided a decent first-order analysis of the behavior of LLL and BKZ. However, they only focused on the *average* behavior and were not perfectly accurate. In this work, we initiate a *second order analysis* of this behavior. We confirm and quantify discrepancies between models and experiments—in particular in the head and tail regions—and study their consequences. We also provide *variations* around the mean and correlations statistics, and study their impact. While mostly based on experiments, by pointing at and quantifying *unaccounted phenomena*, our study sets the ground for a theoretical and predictive understanding of LLL and BKZ performances at the second order.

**Keywords:** Lattice reduction, LLL, BKZ, Cryptanalysis, Statistics.

## 1 Introduction

Lattice reduction is a powerful algorithmic tool for solving a wide range of problems ranging from integer optimization problems and problems from algebra or number theory. Lattice reduction has played a role in the cryptanalysis of cryptosystems not directly related to lattices, and is now even more relevant to quantifying the security of lattice-based cryptosystems [14, 6, 1].

The goal of lattice reduction is to find a basis with short and nearly orthogonal vectors. In 1982, the first polynomial time lattice reduction algorithm, LLL [15], was invented by Lenstra, Lenstra and Lovász. Then, the idea of block-wise reduction appeared and several block-wise lattice reduction algorithms [20, 7, 8, 17] were proposed successively. Currently, BKZ is the most practical lattice reduction algorithm. Schnorr and Euchner first put forward

the original BKZ algorithm in [20]. It is subject to many heuristic optimizations, such as early-abort [12], pruned enumeration [10] and progressive reduction [4, 2]. All such improvements have been combined in the so-called BKZ 2.0 algorithm of Chen and Nguyen [5] (progressive strategy was improved further in later work [2]). Also, plenty of analyses [9, 19, 27, 2, 17] of BKZ algorithms have been made to explore and predict the performance of BKZ algorithms, which provide rough security estimations for lattice-based cryptography.

Despite of their popularity, the behavior of lattice reduction algorithms is still not completely understood. While there are reasonable models (e.g. the Geometric Series Assumption [21] and simulators [5]), there are few studies on the experimental statistical behavior of those algorithms, and they considered rather outdated versions of those algorithms [18, 3, 19]. The accuracy of the current model remains unclear.

This state of affair is quite problematic to evaluate accurately the concrete security level of lattice-based cryptosystem proposal. With the recent calls for post-quantum schemes by the NIST, this matter seems pressing.

*Our Contribution* In this work, we partially address this matter, by proposing a second-order statistical (for random input bases) analysis of the behavior of reduction algorithms in practice, qualitatively and quantitatively. We figure out one more low order term in the predicted average value of several quantities such as the root Hermite factor. Also, we investigate the variation around the average behavior, a legitimate concern raised by Micciancio and Walter [17].

In more details, we experimentally study the logarithms of ratios between two adjacent Gram-Schmidt norms in LLL and BKZ-reduced basis (denoted  $r_i$ 's below). We highlight three ranges for the statistical behavior of the  $r_i$ : the head ( $i \leq h$ ), the body ( $h < i < n - t$ ) and the tail ( $i \geq n - t$ ). The lengths of the head and tail are essentially determined by the blocksize  $\beta$ . In the body range, the statistical behavior of the  $r_i$ 's are similar: this does not only provide new support for the so-called Geometric Series Assumption [21] when  $\beta \ll n$ , but also a refinement of it applicable even when  $\beta \not\ll n$ . We note in particular that the impact of the head on the root Hermite factor is much stronger than the impact of the tail.

We also study the variance and the covariance between the  $r_i$ 's. We observe a local correlation between the  $r_i$ 's. More precisely we observe that  $r_i$  and  $r_{i+1}$  are negatively correlated, inducing a self-stabilizing behavior of those algorithms: the overall variance is less than the sum of local variances.

Then, we measure the half-volume, *i.e.*  $\prod_{i=1}^{\lfloor \frac{n}{2} \rfloor} \|\mathbf{b}_i^*\|$ , a quantity determining the cost of enumeration on reduced basis. By expressing the half-volume using the statistics of the  $r_i$ 's, we determine that the complexity of enumeration on BKZ-reduced basis should be of the form  $2^{an^2 \pm bn^{1.5}}$ : the variation around average (denoted by  $\pm$ ) can impact the speed of enumeration by a super-exponential factor.

At last, we also compare all those experimental results<sup>3</sup> to the simulator [5], and conclude that the simulator can predict the body of the profile and the tail phenomenon qualitatively and quantitatively, but the head phenomenon is not captured. Thus it is necessary to revise the security estimation and refine the simulator.

*Impact* Our work points at several inaccuracies of the current models for the behavior of LLL and BKZ, and quantifies them experimentally. It should be noted that our measured statistics are barely enough to address the question of precise prediction. Many tweaks on those algorithms are typically applied (more aggressive pruning, more subtle progressive reductions, ...) to accelerate them and that would impact those statistics. On the other hand, the optimal parametrization of heuristic tweaks is very painful to reproduce, and not even clearly determined in the literature. We therefore find it preferable to first approach stable versions of those algorithm, and minimize the space of parameters.

We would also not dare to simply guess extrapolation models for those statistics to larger blocksize: this should be the topic of a more theoretical study.

Yet, by pointing out precisely the problematic phenomena, we set the ground for revised models and simulators: our reported statistics can be used to sanity check such future models and simulators.

*Source code* Our experiments heavily rely on the latest improvements of the open-source library `fpLLL` [23], catching up with the state of the art algorithm BKZ 2.0. For convenience, we used the python wrapper `fpYLLL` [24] for `fpLLL`, making our scripts reasonably concise and readable. All our scripts are open-source and available online<sup>4</sup>, for reviewing, reproduction or extension purposes.

## 2 Preliminaries

### 2.1 Notations and Basic Definitions

All vectors are denoted by bold lower case letters and are to be read as row-vectors. Matrices are denoted by bold capital letters. We write a matrix  $\mathbf{B}$  into  $\mathbf{B} = (\mathbf{b}_1, \dots, \mathbf{b}_n)$  where  $\mathbf{b}_i$  is the  $i$ -th row vector of  $\mathbf{B}$ . If  $\mathbf{B} \in \mathbb{R}^{n \times m}$  has full rank  $n$ , the lattice  $\mathcal{L}$  generated by the basis  $\mathbf{B}$  is denoted by  $\mathcal{L}(\mathbf{B}) = \{\mathbf{x}\mathbf{B} \mid \mathbf{x} \in \mathbb{Z}^n\}$ . We denote by  $(\mathbf{b}_1^*, \dots, \mathbf{b}_n^*)$  the Gram-Schmidt orthogonalization of the matrix  $(\mathbf{b}_1, \dots, \mathbf{b}_n)$ . For  $i \in \{1, \dots, n\}$ , we define the orthogonal projection to the span of  $(\mathbf{b}_1, \dots, \mathbf{b}_{i-1})$  as  $\pi_i$ . For  $1 \leq i < j \leq n$ , we denote by  $\mathbf{B}_{[i,j]}$  the local block  $(\pi_i(\mathbf{b}_i), \dots, \pi_i(\mathbf{b}_j))$ , by  $\mathcal{L}_{[i,j]}$  the lattice generated by  $\mathbf{B}_{[i,j]}$ .

The Euclidean norm of a vector  $\mathbf{v}$  is denoted by  $\|\mathbf{v}\|$ . The volume of a lattice  $\mathcal{L}(\mathbf{B})$  is  $\text{vol}(\mathcal{L}(\mathbf{B})) = \prod_i \|\mathbf{b}_i^*\|$ , that is an invariant of the lattice. The first

<sup>3</sup> The variance statistics are not comparable to the simulator [5] whose results are “deterministic”, in the sense that the simulator’s result starting on the Hermite Normal Form of a lattice depends only on the parameters (dimension, volume) of the lattice, and not the randomness of the lattice itself.

<sup>4</sup> Available at <https://github.com/repo-fplll/Statistical-Behavior-of-BKZ>.

minimum of a lattice  $\mathcal{L}$  is the length of a shortest non-zero vector, denoted by  $\lambda_1(\mathcal{L})$ . We use the shorthands  $\text{vol}(\mathbf{B}) = \text{vol}(\mathcal{L}(\mathbf{B}))$  and  $\lambda_1(\mathbf{B}) = \lambda_1(\mathcal{L}(\mathbf{B}))$ .

Given a random variable  $X$ , we denote by  $\mathbf{E}(X)$  its expectation and by  $\mathbf{Var}(X)$  its variance. Also we denote by  $\mathbf{Cov}(X, Y)$  the covariance between two random variables  $X$  and  $Y$ . Let  $\mathbf{X} = (X_1, \dots, X_n)$  be a vector formed by random variables, its covariance matrix is defined by  $\mathbf{Cov}(\mathbf{X}) = (\mathbf{Cov}(X_i, X_j))_{i,j}$ .

## 2.2 Lattice Reduction: in Theory and in Practice

We now recall the definitions of LLL and BKZ reduction. A basis  $\mathbf{B}$  is LLL-reduced with parameter  $\delta \in (\frac{1}{2}, 1]$ , if:

1.  $|\mu_{i,j}| \leq \frac{1}{2}$ ,  $1 \leq j < i \leq n$ , where  $\mu_{i,j} = \langle \mathbf{b}_i, \mathbf{b}_j^* \rangle / \langle \mathbf{b}_j^*, \mathbf{b}_j^* \rangle$  are the Gram-Schmidt orthogonalization coefficients;
2.  $\delta \|\mathbf{b}_i^*\| \leq \|\mathbf{b}_{i+1}^* + \mu_{i+1,i} \mathbf{b}_i^*\|$ , for  $1 \leq i < n$ .

A basis  $\mathbf{B}$  is BKZ-reduced with parameter  $\beta \geq 2$  and  $\delta \in (\frac{1}{2}, 1]$ , if:

1.  $|\mu_{i,j}| \leq \frac{1}{2}$ ,  $1 \leq j < i \leq n$ ;
2.  $\delta \|\mathbf{b}_i^*\| \leq \lambda_1(\mathcal{L}_{[i, \min(i+\beta-1, n)]})$ , for  $1 \leq i < n$ .

Note that we follow the definition of BKZ reduction from [20] which is a little different from the first notion proposed by Schnorr [22]. We also recall that, as proven in [20], LLL is equivalent to BKZ<sub>2</sub>. Typically, LLL and BKZ are used with *Lovász parameter*  $\delta = \sqrt{0.99}$  and so will we.

For high dimensional lattices, running BKZ with a large blocksize is very expensive. Heuristics improvements were developed, and combined by Chen and Nguyen [5], advertised as BKZ 2.0.<sup>5</sup> In this paper, we report on pure BKZ behavior to avoid perturbations due to heuristic whenever possible. Yet we switch to BKZ 2.0 to reach larger blocksizes when deemed relevant.

The two main improvements in BKZ 2.0 are called *early-abort* and *pruned enumeration*. As proven in [12], the output basis of BKZ algorithm with blocksize  $\beta$  would be of an enough good quality after  $C \cdot \frac{n^2}{\beta^2} \left( \log n + \log \log \max \frac{\|\mathbf{b}_i^*\|}{\text{vol}(\mathcal{L})^{1/n}} \right)$  tours, where  $C$  is a small constant. In our experiments of BKZ 2.0, we chose different  $C$  and observed its effect on the final basis. We also applied the pruning heuristic to speed-up enumeration, but chose a conservative success probability (95%) without re-randomization to avoid altering the quality of the output. The preprocessing-pruning strategies were optimized using the strategizer [25] of `fpIII/fpyIII`.

Given a basis  $\mathbf{B}$  of an  $n$ -dimensional lattice  $\mathcal{L}$ , we denote by  $\mathbf{rhf}(\mathbf{B})$  the root Hermite factor of  $\mathbf{B}$ , defined by  $\mathbf{rhf}(\mathbf{B}) = \left( \frac{\|\mathbf{b}_1\|}{\text{vol}(\mathcal{L})^{1/n}} \right)^{1/n}$ . The root Hermite factor is a common measurement of the reducedness of a basis.

<sup>5</sup> Further improvements were recently put forward [2], but are beyond the scope of this paper.

Let us define the sequence  $\{r_i(\mathbf{B})\}_{1 \leq i \leq n-1}$  of an  $n$ -dimensional lattice basis  $\mathbf{B} = (\mathbf{b}_1, \dots, \mathbf{b}_n)$  such that  $r_i(\mathbf{B}) = \ln(\|\mathbf{b}_i^*\|/\|\mathbf{b}_{i+1}^*\|)$ . The root Hermite factor  $\mathbf{rhf}(\mathbf{B})$  can be expressed in terms of the  $r_i(\mathbf{B})$ 's:

$$\mathbf{rhf}(\mathbf{B}) = \exp\left(\frac{1}{n^2} \sum_{1 \leq i \leq n-1} (n-i)r_i(\mathbf{B})\right). \quad (1)$$

Intuitively, the sequence  $\{r_i(\mathbf{B})\}_{1 \leq i \leq n-1}$  characterizes how fast the sequence  $\{\|\mathbf{b}_i^*\|\}$  decreases. Thus Equation (1) provides an implication between the fact that the  $\|\mathbf{b}_i^*\|$ 's don't decrease too fast and the fact that the root Hermite factor is small. For reduced bases, the  $r_i(\mathbf{B})$ 's are of certain theoretical upper bounds. However, it is well known that experimentally, the  $r_i(\mathbf{B})$ 's tend to be much smaller than the theoretical bounds in practice.

From a practical perspective, we are more interested in the behavior of the  $r_i(\mathbf{B})$ 's for random lattices. The standard notion of random real lattices of given volume is based on Haar measures of classical groups. As shown in [11], the uniform distribution over integer lattices of volume  $V$  converges to the distribution of random lattices of unit volume, as  $V$  grows to infinity. In our experiments, we followed the sampling procedure of the lattice challenges<sup>6</sup>: its volume is a random prime of bit-length  $10n$  and its Hermite normal form is sampled uniformly once its volume is determined. Also, we define a random LLL (resp.  $\text{BKZ}_\beta$ )-reduced basis as the basis outputted by LLL (resp.  $\text{BKZ}_\beta$ ) applied to a random lattice given by its Hermite normal form, as described above. To speed up convergence, following a simplified progressive strategy [4, 2], we run BKZ (resp. BKZ 2.0) with blocksize  $\beta = 2, 4, 6, \dots$  (resp.  $\beta = 2, 6, 10, \dots$ ) progressively from the Hermite normal form of a lattice.

We treat the  $r_i(\mathbf{B})$ 's as random variables (under the randomness of the lattice basis before reduction). For any  $i \in \{1, \dots, n-1\}$ , we denote by  $r_i(\beta, n)$  the random variable  $r_i(\beta, n) = r_i(\mathbf{B})$ , where  $\mathbf{B}$  is a random  $\text{BKZ}_\beta$ -reduced basis, and by  $\mathbb{D}_i(\beta, n)$  the distribution of  $r_i(\beta, n)$ . When  $\beta$  and  $n$  are clear from context, we simply write  $r_i$  for  $r_i(\beta, n)$ .

### 2.3 Heuristics on Lattice Reduction

*Gaussian Heuristic* The Gaussian Heuristic, denoted by GAUSS, says that, for “any reasonable” subset  $K$  of the span of the lattice  $\mathcal{L}$ , the number of lattice points inside  $K$  is approximately  $\text{vol}(K)/\text{vol}(\mathcal{L})$ . Let the volume of  $n$ -dimensional unit ball be  $V_n(1) = \frac{\pi^{n/2}}{\Gamma(n/2+1)}$ . A prediction derived from GAUSS is that  $\lambda_1(\mathcal{L}) \approx \text{vol}(\mathcal{L})^{1/n} \cdot \text{GH}(n)$  where  $\text{GH}(n) = V_n(1)^{-1/n}$ , which is accurate for random lattices. As suggested in [13, 10], GAUSS is a valuable heuristic to estimate the cost and quality of various lattice algorithms.

<sup>6</sup> <https://latticechallenge.org/svp-challenge>

*Random Local Block* In [5], Chen and Nguyen suggested the following modeling assumption, seemingly accurate for large enough block sizes:

**Assumption 1** [*RAND<sub>n,β</sub>*] Let  $n, \beta \geq 2$  be integers. For a random  $BKZ_\beta$ -reduced basis of a random  $n$ -dimensional lattice, most local block lattices  $\mathcal{L}_{[i, i+\beta-1]}$  behave like a random  $\beta$ -dimensional lattice where  $i \in \{1, \dots, n+1-\beta\}$ .

By  $RAND_{n,\beta}$  and GAUSS, one can predict the root Hermite factor of local blocks:  $\mathbf{rhf}(\mathbf{B}_{[i, i+\beta-1]}) \approx \text{GH}(\beta)^{\frac{1}{\beta}}$ .

*Geometric Series Assumption* In [21], Schnorr first proposed the Geometric Series Assumption, denoted by GSA, which says that, in typical reduced basis  $\mathbf{B}$ , the sequence  $\{\|\mathbf{b}_i^*\|\}_{1 \leq i \leq n}$  looks like a geometric series (while GAUSS provides the exact value of this geometric ratio). GSA provides a simple description of Gram-Schmidt norms and then leads to some estimations of Hermite factor and enumeration complexity [9, 10]. When it comes to  $\{r_i(\mathbf{B})\}_{1 \leq i \leq n-1}$ , GSA implies that the  $r_i(\mathbf{B})$ 's are supposed to be almost equal to each others. However, GSA is not so perfect, because the first and last  $\mathbf{b}_i^*$ 's usually violate it [3]. The behavior in the tail is well explained, and can be predicted and simulated [5].

### 3 Head and Tail

In [3, 5], it was already claimed that for a  $BKZ_\beta$ -reduced basis  $\mathbf{B}$ , GSA doesn't hold in the first and last indices. We call this phenomenon "Head and Tail", and provide detailed experiments. Our experiments confirm that GSA holds in a strong sense in the body of the basis (*i.e.* outside of the head and tail regions). Precisely, the distributions of  $r_i$ 's are similar in that region, not only their averages. We also confirm the violations of GSA in the head and the tail, quantify them, and exhibit that they are independent of the dimension  $n$ .

As a conclusion, we shall see that the head and tail have only small impacts on the root Hermite factor when  $n \gg \beta$ , but also that they can also be quantitatively handled when  $n \not\gg \beta$ . We notice that the head has in fact a stronger impact than the tail, which emphasizes the importance of finding models or simulators that capture this phenomenon, unlike the current ones that only capture the tail [5].

#### 3.1 Experiments

We ran  $BKZ$  on many random input lattices and report on the distribution of each  $r_i$ . We first plot the average and the variance of  $r_i$  for various block sizes  $\beta$  and dimensions  $n$  in Figure 1. By superposing with proper alignment curves for the same  $\beta$  but various  $n$ , we notice that the head and tail behavior doesn't depend on the dimension  $n$ , but only on the relative index  $i$  (resp.  $n-i$ ) in the head (resp. the tail). A more formal statement will be provided in Claim 1.

We also note that inside the body (*i.e.* outside both the head and the tail) the mean and the variance of  $r_i$  do not seem to depend on  $i$ , and are tempted to conclude that the distribution itself doesn't depend on  $i$ . To give further evidence

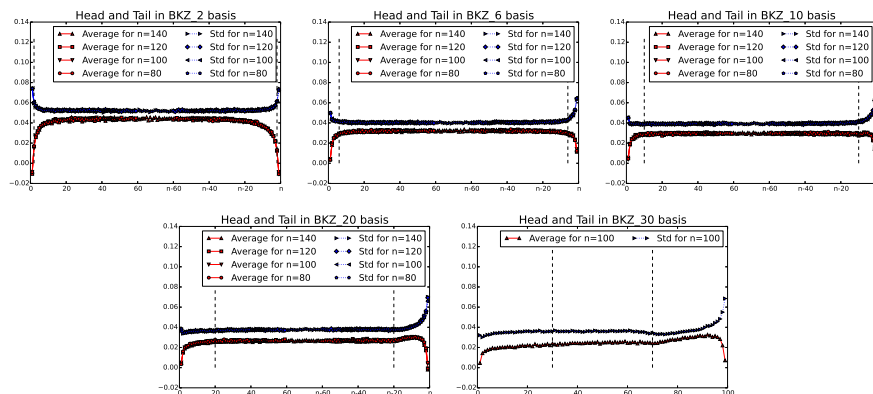


**Fig. 1.** Average value and standard deviation of  $r_i$  as a function of  $i$ . Experimental values measure over 5000 samples of random  $n$ -dimensional BKZ bases for  $n = 80, 100, 120, 140$ . First halves  $\{r_i\}_{i \leq (n-1)/2}$  are left-aligned while last halves  $\{r_i\}_{i > (n-1)/2}$  are right-aligned so to highlight heads and tails. Dashed lines mark indices  $\beta$  and  $n - \beta$ . Due to the expensive cost of running BKZ<sub>30</sub> on high dimensional lattices, we only present the result of BKZ<sub>30</sub> for  $n = 100$  mostly as a reference to test the accuracy of the simulator, see Section 6.

of this stronger claim, we ran the Kolmogorov-Smirnov test [16] on samples of  $r_i$  and  $r_j$  for varying  $i, j$ . The results are depicted on Figure 2, and confirm this stronger claim.

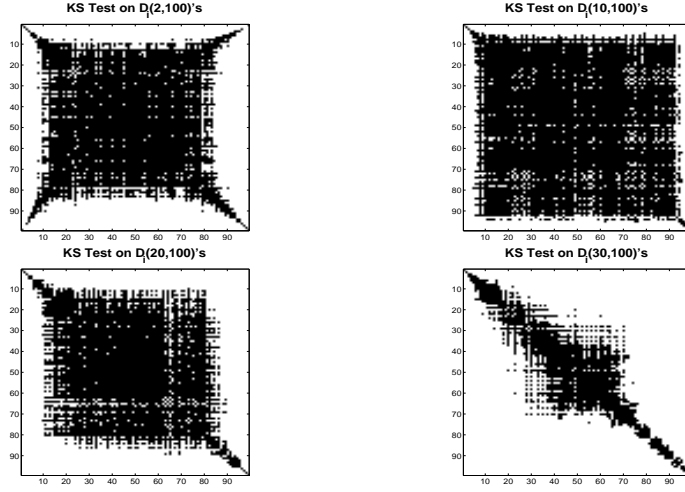


**Fig. 2.** Kolmogorov-Smirnov Test with significance level 0.05 on all  $\mathbb{D}_i(\beta, 100)$ 's calculated from 5000 samples of random 100-dimensional BKZ bases with blocksize  $\beta = 2, 10, 20, 30$  respectively. A black pixel at position  $(i, j)$  marks the fact that the pair of distributions  $\mathbb{D}_i(\beta, 100)$  and  $\mathbb{D}_j(\beta, 100)$  passed Kolmogorov-Smirnov Test, *i.e.* two distributions are close.

### 3.2 Conclusion

From the experiments above, we allow ourselves to the following conclusion.

**Experimental Claim 1** *There exist two functions  $h, t : \mathbb{N} \rightarrow \mathbb{N}$ , such that, for all  $n, \beta \in \mathbb{N}$ , and when  $n \geq h(\beta) + t(\beta) + 2$  :*

1. *When  $i \leq h(\beta)$ ,  $\mathbb{D}_i(\beta, n)$  depends on  $i$  and  $\beta$  only:  $\mathbb{D}_i(\beta, n) = \mathbb{D}_i^h(\beta)$*
2. *When  $h(\beta) < i < n - t(\beta)$ ,  $\mathbb{D}_i(\beta, n)$  depends on  $\beta$  only:  $\mathbb{D}_i(\beta, n) = \mathbb{D}^b(\beta)$*
3. *When  $i \geq n - t(\beta)$ ,  $\mathbb{D}_i(\beta, n)$  depends on  $n - i$  and  $\beta$  only:  $\mathbb{D}_i(\beta, n) = \mathbb{D}_{n-i}^t(\beta)$*

*Remark 1.* We only make this claim for basis that have been fully BKZ-reduced. Indeed, as we shall see later, we obtained experimental clues that this claim would not hold when the early-abort strategy is applied. More precisely, the head and tail phenomenon is getting stronger as we apply more tours (see Figure 4).

From now on, we may omit the index  $i$  when speaking of the distribution of  $r_i$ , implicitly implying that the only indices considered are such that  $h(\beta) < i < n - t(\beta)$ . The random variable  $r$  depends on blocksize  $\beta$  only, hence we introduce two functions of  $\beta$ ,  $e(\beta)$  and  $v(\beta)$ , to denote the expectation and variance of  $r$  respectively. Also, we denote by  $r_i^{(h)}$  (resp.  $r_{n-i}^{(t)}$ ) the  $r_i$  inside the head (resp. tail), and by  $e_i^{(h)}(\beta)$  and  $v_i^{(h)}(\beta)$  (resp.  $e_{n-i}^{(t)}(\beta)$  and  $v_{n-i}^{(t)}(\beta)$ ) the expectation and variance of  $r_i^{(h)}$  (resp.  $r_{n-i}^{(t)}$ ).

We conclude by a statement on the impacts of the head and tail on the logarithmic average root Hermite factor:

**Corollary 1.** For a fixed blocksize  $\beta$ , and as the dimension  $n$  grows, it holds that

$$\mathbf{E}(\ln(\mathbf{rhf}(\mathbf{B}))) = \frac{1}{2}e(\beta) + \frac{d(\beta)}{n} + O\left(\frac{1}{n^2}\right), \quad (2)$$

where  $d(\beta) = \sum_{i \leq h} e_i^{(h)}(\beta) - (h + \frac{1}{2})e(\beta)$ .

Corollary 1 indicates that the impacts on the average root Hermite factor from the head and tail are decreasing. In particular, the tail has a very little effect  $O\left(\frac{1}{n^2}\right)$  on the average root Hermite factor. The impact of the head  $d(\beta)/n$ , which hasn't been quantified in earlier work, is *—perhaps surprisingly—* asymptotically larger. We include the proof of Corollary 1 in Appendix B.

Below, Figures 3 and 4 provide experimental measure of  $e(\beta)$  and  $d(\beta)$  from 5000 random 100-dimensional  $\text{BKZ}_\beta$ -reduced bases. We note that the lengths of the head and tail seem about the maximum of 15 and  $\beta$ . Thus we set  $h(\beta) = t(\beta) = \max(15, \beta)$  simply, which affects the measure of  $e(\beta)$  and  $d(\beta)$  little. For the average  $e(2) \approx 0.043$  we recover the experimental root Hermite factor of LLL  $\mathbf{rhf}(\mathbf{B}) = \exp(0.043/2) \approx 1.022$ , compatible with many other experiments [9].

To extend the curves, we also plot the experimental measure of  $e(\beta)$  and  $d(\beta)$ <sup>7</sup> from 20 random 180-dimensional  $\text{BKZ}_\beta$  2.0 bases with bounded four number  $\left[ C \cdot \frac{n^2}{\beta^2} \left( \log n + \log \log \max \frac{\|\mathbf{b}_i^*\|}{\text{vol}(\mathcal{L})^{1/n}} \right) \right]$ . It shows that the qualitative behavior of  $\text{BKZ}$  2.0 is different from full- $\text{BKZ}$  not only the quantitative one: there is a bump<sup>8</sup> in the curve of  $e(\beta)$  when  $\beta \in [22, 30]$ . Considering that the success probability for the SVP enumeration was set to 95%, the only viable explanation for this phenomenon in our  $\text{BKZ}$  2.0 experiments is the early-abort strategy: the shape of the basis is not so close to the fix-point.

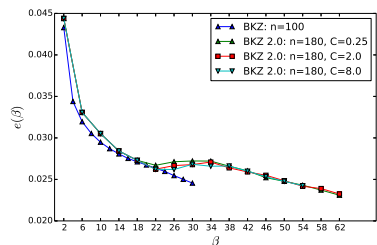


**Fig. 3.** Experimental measure of  $e(\beta)$

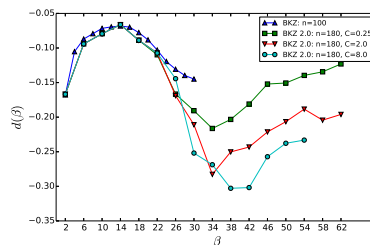


**Fig. 4.** Experimental measure of  $d(\beta)$

<sup>7</sup> For  $\text{BKZ}$  2.0, the distributions of the  $r_i$ 's inside the body may not be identical, thus we just calculate the mean of those  $r_i$ 's as a measure of  $e(\beta)$ .

<sup>8</sup> Yet the quality of the basis does not decrease with  $\beta$  in this range, as the bump on  $e(\beta)$  is more than compensated by the decrease in  $d(\beta)$ .

## 4 Local correlations and global variance

In the previous section, we have classified the  $r_i$ 's and established a connection between the average of the root Hermite factor and the function  $e(\beta)$ . Now we are to report on the (co-)variance of the  $r_i$ 's. Figure 5 shows the experimental measure of local variances, *i.e.* variances of the  $r_i$ 's inside the body, but it is not enough to deduce the global variance, *i.e.* the variance of the root Hermite factor. We still need to understand more statistics, namely the covariances among these  $r_i$ 's. Our experiments indicate that local correlations —*i.e.* correlations between  $r_i$  and  $r_{i+1}$ — are negative and other correlations seem to be zero. Moreover, we confirm the tempting hypothesis that local correlations inside the body are all equal and independent of the dimension  $n$ .

Based on these observations, we then express the variance of the logarithm of root Hermite factor for fixed  $\beta$  and increasing  $n$  asymptotically, and quantify the self-stability of LLL and BKZ algorithms.

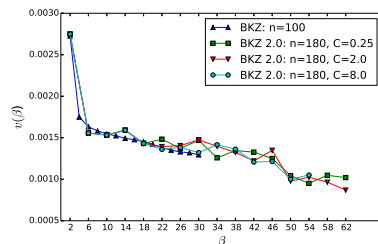
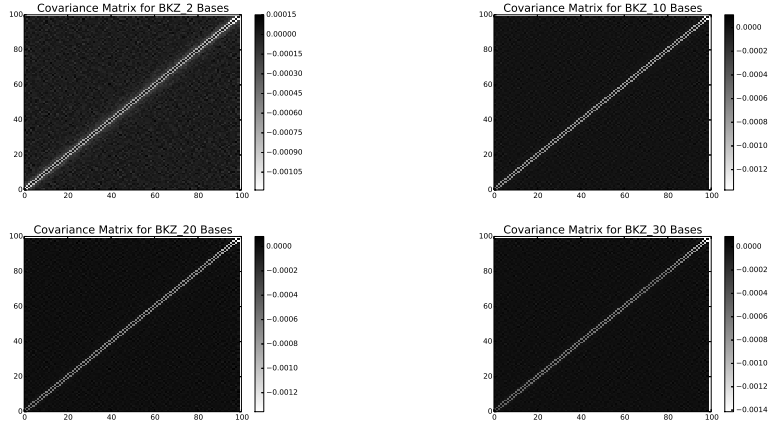


Fig. 5. Experimental measure of  $v(\beta)$

### 4.1 Experiments

Let  $\mathbf{r} = (r_1, \dots, r_{n-1})$  be the random vector formed by random variables  $r_i$ 's. We profile the covariance matrices  $\mathbf{Cov}(\mathbf{r})$  for 100-dimensional lattices with BKZ reduction of different blocksizes in Figure 6. The diagonal elements in covariance matrix correspond to the variances of the  $r_i$ 's which we have studied before. Thus we set all diagonal elements to 0 to enhance contrast. We discover that the elements on the second diagonals, *i.e.*  $\mathbf{Cov}(r_i, r_{i+1})$ 's, are significantly negative and other elements seems very close to 0. We call the  $\mathbf{Cov}(r_i, r_{i+1})$ 's local covariances.

We then plot measured local covariances in Figure 7. Comparing these curves for various dimensions  $n$ , we notice that the head and tail parts almost coincide, and the local covariances inside the body seem to depend on  $\beta$  only, we will denote this value by  $c(\beta)$ . We also plot the curves of the  $\mathbf{Cov}(r_i, r_{i+2})$ 's in Figure 7 and note that the curves for the  $\mathbf{Cov}(r_i, r_{i+2})$ 's are horizontal with a value about 0. For other  $\mathbf{Cov}(r_i, r_{i+d})$ 's with larger  $d$ , the curves virtually overlap that for the  $\mathbf{Cov}(r_i, r_{i+2})$ 's. For readability, larger values of  $d$  are not



**Fig. 6.** Covariance matrices of  $\mathbf{r}$ . Experimental values measure over 5000 samples of random 100-dimensional BKZ bases with blocksize  $\beta = 2, 10, 20, 30$  respectively. The pixel at coordinates  $(i, j)$  corresponds to the covariance between  $r_i$  and  $r_j$ .

plotted. One thing to be noted is that the case for blocksize  $\beta = 2$  is an exception. On one hand, the head and tail of the local covariances in  $\text{BKZ}_2$  basis bend in the opposite directions, unlike for larger  $\beta$ . In particular, the  $\mathbf{Cov}(r_i, r_{i+2})$ 's in  $\text{BKZ}_2$  basis are not so close to 0, but are nevertheless significantly smaller than the local covariances  $\mathbf{Cov}(r_i, r_{i+1})$ . That indicates some differences between LLL and BKZ.

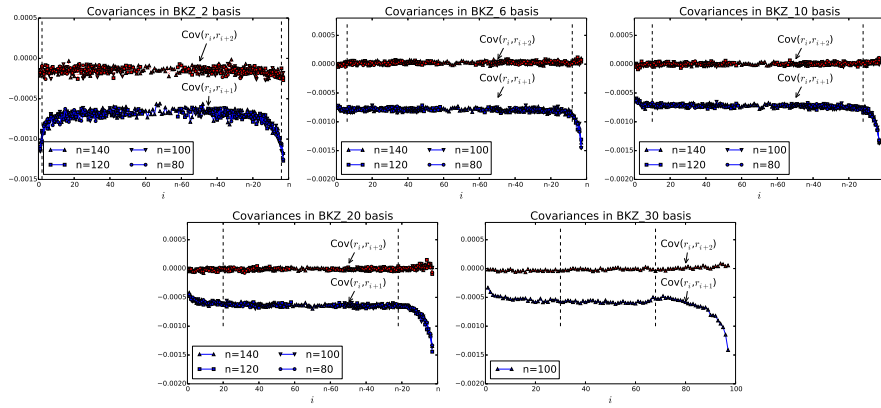


**Fig. 7.**  $\text{Cov}(r_i, r_{i+1})$  and  $\text{Cov}(r_i, r_{i+2})$  as a function of  $i$ . Experimental values measured over 5000 samples of random  $n$ -dimensional BKZ bases for  $n = 80, 100, 120, 140$ . The blue curves denote the  $\text{Cov}(r_i, r_{i+1})$ 's and the red curves denote the  $\text{Cov}(r_i, r_{i+2})$ 's. For same dimension  $n$ , the markers in two curves are identical. First halves are left aligned while last halves  $\{\text{Cov}(r_i, r_{i+1})\}_{i > (n-2)/2}$  and  $\{\text{Cov}(r_i, r_{i+2})\}_{i > (n-3)/2}$  are right aligned so to highlight heads and tails. Dashed lines mark indices  $\beta$  and  $n - \beta - 2$ .

Also, we calculate the average of  $(n - 2 \max(15, \beta))$  middle local covariances as an approximation of  $c(\beta)$  for different  $n$  and plot the evolution of  $c(\beta)$  in Figure 8. The curves for different dimensions seem to coincide, which provides another evidence to support that the local covariances inside the body don't depend on  $n$  indeed. To determine the minimum of  $c(\beta)$ , we ran a batch of BKZ with  $\beta = 2, 3, 4, 5, 6$  separately. We note that  $c(\beta)$  increases with  $\beta$  except for  $c(3) < c(2)$ , which is another difference between LLL and BKZ.

*Remark 2.* To obtain a precise measure of covariances, we need enough samples and thus the extended experimental measure of  $c(\beta)$  is not given. Nevertheless, it seems that, after certain number of tours, local covariances of BKZ 2.0 bases still tend to be negative but other covariances tend to zero.

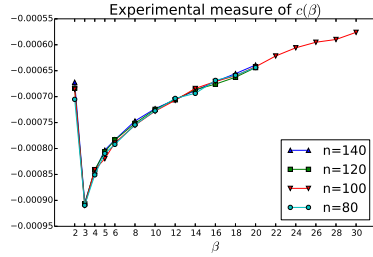


**Fig. 8.** Experimental measure of the evolution of  $c(\beta)$  calculated from 5000 samples of random BKZ bases in different dimension  $n$  respectively.

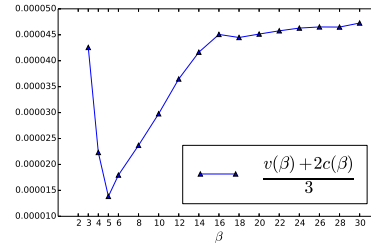


**Fig. 9.** Experimental measure of  $\frac{v(\beta)+2c(\beta)}{3}$ . The data point for  $\beta = 2$ ,  $\frac{v(2)+2c(2)}{3} \approx 0.00045$  was clipped out, being 10 times larger than all other values.

## 4.2 Conclusion

From above experimental observations, we now arrive at the following conclusion.

**Experimental Claim 2** Let  $h$  and  $t$  be the two functions defined in Claim 1. For all  $n \in \mathbb{N}$  and  $\beta > 2$  such that  $n \geq h(\beta) + t(\beta) + 2$ :

1. When  $|i - j| > 1$ ,  $r_i$  and  $r_j$  are not correlated:  $\mathbf{Cov}(r_i, r_j) = 0$
2. When  $|i - j| = 1$ ,  $r_i$  and  $r_j$  are negatively correlated:  $\mathbf{Cov}(r_i, r_j) < 0$ . More specifically:
  - When  $i \leq h(\beta)$ ,  $\mathbf{Cov}(r_i, r_{i+1})$  depends on  $i$  and  $\beta$  only:  $\mathbf{Cov}(r_i, r_{i+1}) = c_i^h(\beta)$
  - When  $h(\beta) < i < n - t(\beta)$ ,  $\mathbf{Cov}(r_i, r_{i+1})$  depends on  $\beta$  only:  $\mathbf{Cov}(r_i, r_{i+1}) = c(\beta)$
  - When  $i \geq n - t(\beta)$ ,  $\mathbf{Cov}(r_i, r_{i+1})$  depends on  $n - i$  and  $\beta$  only:  $\mathbf{Cov}(r_i, r_{i+1}) = c_{n-i}^t(\beta)$

One direct consequence derives from the above experimental claim is that the global variance, *i.e.* the variance of the logarithm of root Hermite factor, converges to 0 as  $\Theta(1/n)$ , where the hidden constant is determined by  $\beta$ :

**Corollary 2.** For a fixed blocksize  $\beta$ , and as the dimension  $n$  grows, it holds that

$$\mathbf{Var}(\ln(\mathbf{rhf}(\mathbf{B}))) = \frac{1}{3n}v(\beta) + \frac{2}{3n}c(\beta) + O\left(\frac{1}{n^2}\right). \quad (3)$$

The proof of Corollary 2 is given in Appendix C. Note that the assumption that all  $\mathbf{Cov}(r_i, r_{i+d})$ 's with  $d > 1$  equal 0 may not be exactly true. However, the  $\mathbf{Cov}(r_i, r_{i+d})$ 's converge to 0 quickly as  $d$  increases, hence we may assert that the sum  $\sum_{d=1}^{n-1-i} \mathbf{Cov}(r_i, r_{i+d})$  converge with  $n$  for fixed  $\beta$  and  $i$  inside the body. Then we still can conclude that  $\mathbf{Var}(\ln(\mathbf{rhf}(\mathbf{B}))) = O(\frac{1}{n})$ . The faster the  $\mathbf{Cov}(r_i, r_{i+d})$ 's converges to 0 as  $d$  grows, the more accurate our above approximation is. The experimental measure of  $\frac{v(\beta)+2c(\beta)}{3}$  is shown in Figure 9 and  $\frac{v(\beta)+2c(\beta)}{3}$  seems to converge to a finite value  $\approx 5 \times 10^{-5}$  as  $\beta$  grows.

## 5 Half Volume

We shall now study statistics on the half-volume,  $H(\mathbf{B}) = \prod_{i=1}^{\lfloor \frac{n}{2} \rfloor} \|\mathbf{b}_i^*\|$ , of a random BKZ-reduced basis  $\mathbf{B}$ . As claimed in [10], the nodes in the enumeration tree at the depths around  $\frac{n}{2}$  contribute the most to the total node number, for both full and regular pruned enumerations. Typically, the enumeration radius  $R$  is set to  $c\sqrt{n} \cdot \text{vol}(\mathbf{B})^{\frac{1}{n}}$  for some constant  $c > 0$ , e.g.  $R = 1.05 \cdot \text{GH}(n) \cdot \text{vol}(\mathbf{B})^{\frac{1}{n}}$ , the number of nodes in the  $\lfloor \frac{n}{2} \rfloor$  level is approximately proportional to  $\frac{H(\mathbf{B})}{\text{vol}(\mathbf{B})^{\frac{1}{2} \cdot \frac{1}{n}}}$ , making the half-volume a good estimator for the cost of enumeration. Those formulas have to be amended in case pruning is used (see [10]), but the half-volume remains a good indicator of the cost of enumeration.

Let  $\mathbf{h}\mathbf{v}(\beta, n)$  be the random variable  $\ln(H(\mathbf{B})) - \frac{\lfloor \frac{n}{2} \rfloor}{n} \ln(\text{vol}(\mathbf{B}))$  where  $\mathbf{B}$  is a random  $\text{BKZ}_\beta$ -reduced basis. By the above experimental claims, we conclude the following result. The proof is shown in Appendix D.

**Corollary 3 (Under previous experimental claims).** *For a fixed blocksize  $\beta$ , let  $n$  be an integer such that  $n > 2 \max(h(\beta), t(\beta))$ . Then, as the dimension  $n$  grows, it holds that*

$$\mathbf{E}(\mathbf{h}\mathbf{v}(\beta, n)) = \frac{n^2}{8} e(\beta) + d'(\beta) + O\left(\frac{1}{n}\right), \quad (4)$$

where  $d'(\beta) = \sum_{i \leq h} \frac{i}{2} (e_i^{(h)}(\beta) - e(\beta)) + \sum_{i \leq t} \frac{i}{2} (e_i^{(t)} - e(\beta)) - \frac{1}{4} \lfloor \frac{n}{2} \rfloor e(\beta)$ , and

$$\mathbf{Var}(\mathbf{h}\mathbf{v}(\beta, n)) = \frac{n^3}{48} (v(\beta) + 2c(\beta)) + O(n). \quad (5)$$

Assuming heuristically that the variation around the average of  $\mathbf{h}\mathbf{v}$  follows a Normal law, Corollary 3 implies that the complexity of enumeration on a random  $n$ -dimensional  $\text{BKZ}_\beta$ -reduced basis should be of the shape

$$\exp(n^2 x(\beta) + y(\beta) \pm n^{1.5} l \cdot z(\beta)) \quad (6)$$

except a fraction at most  $\exp(-l^2/2)$  of random bases, where

$$x(\beta) = \frac{e(\beta)}{8}, \quad y(\beta) = d'(\beta), \quad z(\beta) = \sqrt{\frac{v(\beta) + 2c(\beta)}{48}} \quad (7)$$

and where the term  $\pm n^{1.5} l \cdot z(\beta)$  accounts for variation around the average behavior. In particular, the contribution of the variation around the average remains asymptotically negligible compared to the main  $\exp(\Theta(n^2))$  factor, it still introduces a super-exponential factor, that can make one particular attempt much cheaper or much more expensive in practice. It means that it could be beneficial in practice to rely partially on luck, restarting BKZ without trying enumeration when the basis is unsatisfactory.

The experimental measure of  $8x(\beta)$  and  $16z(\beta)^2$  has been shown in Figure 3 and 9 respectively. We now exhibit the experimental measure of  $y(\beta)$

in Figure 10. Despite the curves for BKZ 2.0 are not smooth, it seems that  $y(\beta)(= d'(\beta))$  would increase with  $\beta$  when  $\beta$  is large. However, comparing to  $n^2x(\beta)$ , the impact of  $y(\beta)$  on the half-volume is still much weaker.<sup>9</sup>

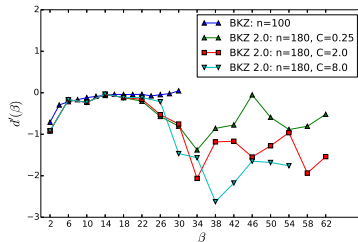


Fig. 10. Experimental measure of  $y(\beta)(= d'(\beta))$

## 6 Performance of Simulator

In [5], Chen and Nguyen proposed a simulator to predict the behavior of BKZ. For large  $\beta$ , the simulator can provide a reasonable prediction of average profile, *i.e.*  $\left\{ \log \left( \frac{\|\mathbf{b}_i^*\|}{\text{vol}(\mathcal{L})^{1/n}} \right) \right\}_{i=1}^n$ . In this section, we will further report on the performance of the simulator qualitatively and quantitatively. Our experiments confirm that the tail still exists in the simulated result and fits the actual measure, but the head phenomenon is not captured by the simulator, affecting its accuracy for cryptanalytic prediction.

To make the simulator<sup>10</sup> coincide with the actual algorithm, we set the parameter  $\delta = \sqrt{0.99}$  and applied a similar progressive strategy<sup>11</sup>. The maximum tour number corresponds to the case that  $C = 0.25$  in [12], but the simulator always terminates after a much smaller number of tours.

### 6.1 Experiments

We ran simulator on several sequences of different dimensions and plot the average values of  $r_i$ 's in Figure 11. An apparent tail remains in the simulated result and the length of its most significant part is about  $\beta$  despite a slim stretch. However, there is no distinct head, which does not coincide with the actual behavior: the head shape appears after a few tours of BKZ or BKZ 2.0. Still, the  $r_i$ 's inside the body share similar values, in accordance with GSA and experiments.

<sup>9</sup> The impacts of the  $r_i$ 's inside the head and tail will still be significant when  $\beta = O(n)$ .

<sup>10</sup> We worked on an open-source BKZ simulator [26], with minor modifications.

<sup>11</sup> In simulation, the initial profile sequence is set to  $(10(n-1), -10, \dots, -10)$  and then we started from blocksize 6 and progressively ran simulator by step 2 (or 4 to simulate BKZ 2.0.). There seems to be something wrong when starting with BKZ<sub>2</sub>.

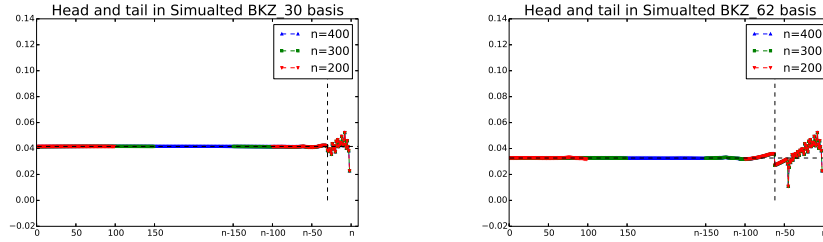


**Fig. 11.** Average value of  $r_i$  calculated by simulator. First halves are left aligned while last halves  $\{r_i\}_{i > (n-1)/2}$  are right aligned so to highlight heads and tails. The vertical dashed line marks the index  $n - \beta$  and the horizontal dashed line is used for contrast.

We now compare the average experimental behavior with the simulated result. Note that the simulator is not fed with any randomness, so it does not make sense to consider variance in this comparison.

Figure 12 illustrates the comparison on  $e(\beta)$ . For small blocksize  $\beta$ , the simulator does not work well, but, as  $\beta$  increases, the simulated measure of  $e(\beta)$  seems close to the experimental measure and both measures converge to the prediction  $\ln\left(\text{GH}(\beta)^{\frac{2}{\beta-1}}\right)$ .

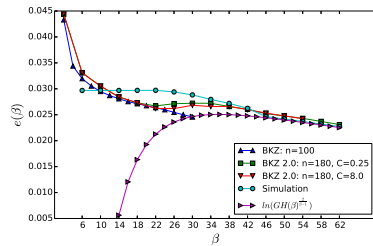


**Fig. 12.** Comparison on  $e(\beta)$

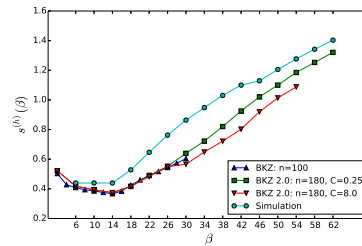


**Fig. 13.** Comparison on  $s^{(h)}(\beta)$

Finally, we consider the two functions  $d(\beta)$  and  $d'(\beta)$  that are relevant to the averages of the logarithms of the root Hermite factor and the complexity of enumeration and defined in Corollary 1 and 3 respectively. To better understand the difference, we compared the following terms  $s^{(h)}(\beta) = \sum_{i \leq h} e_i^{(h)}(\beta)$ ,  $w^{(h)}(\beta) = \sum_{i \leq h} \frac{i}{2} e_i^{(h)}(\beta)$  and  $w^{(t)}(\beta) = \sum_{i \leq t} \frac{i}{2} e_i^{(t)}$  respectively, where we set  $h(\beta) = t(\beta) = \max(15, \beta)$  as before. Indeed, combined with  $e(\beta)$ , these three terms determine  $d(\beta)$  and  $d'(\beta)$ .

From Figure 13, we observe that the simulated measure of  $s^{(h)}(\beta)$  is greater than the experimental measure, which is caused by the lack of the head. The similar inaccuracy exists as well with respect to  $w^{(h)}(\beta)$  as shown in Figure 14.

The experimental measure of  $e(\beta)$  is slightly greater than the simulated measure and thus the  $e_i^{(h)}(\beta)$ 's of greater weight may compensate somewhat the lack of the head. After enough tours, the head phenomenon is highlighted and yet the body shape almost remains the same so that the simulator still cannot predict  $w^{(h)}(\beta)$  precisely. Figure 15 indicates that the simulator could predict  $w^{(t)}(\beta)$  precisely for both large and small block sizes and therefore the HKZ-shaped tail model is reasonable.

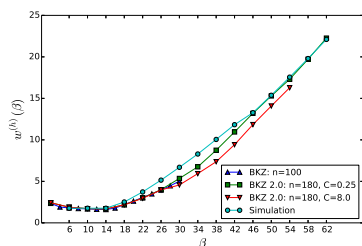


Fig. 14. Comparison on  $w^{(h)}(\beta)$

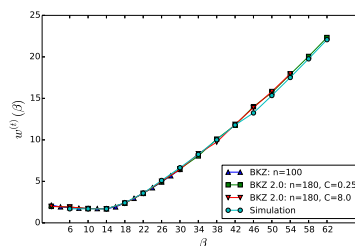


Fig. 15. Comparison on  $w^{(t)}(\beta)$

## 6.2 Conclusion

Chen and Nguyen's simulator gives an elementary profile for random  $BKZ_{\beta}$ -reduced bases with large  $\beta$ : both body and tail shapes are reflected well in the simulation result qualitatively and quantitatively. However, the head phenomenon is not captured by this simulator, and thus the first  $\|\mathbf{b}_i^*\|$ 's are not predicted accurately. Consequently, the simulator may not provide exact predictions for some metrics, e.g. Hermite factor, and related security estimations need to be refined.

Understanding the main cause of the head phenomenon, modeling it and refining the simulator to include it seems an interesting and important problem, which we leave to the future work. It would also be interesting to introduce some randomness in the simulator, so to properly predict variance around the mean behavior.

## References

- [1] Alkim, E., Ducas, L., Pöppelmann, T., Schwabe, P.: Post-quantum key exchange—a new hope. In: *USENIX Security 16*. (2016) 327–343
- [2] Aono, Y., Wang, Y., Hayashi, T., Takagi, T.: Improved progressive BKZ algorithms and their precise cost estimation by sharp simulator. In: *EUROCRYPT 2016*. (2016) 789–819
- [3] Buchmann, J., Ludwig, C.: Practical lattice basis sampling reduction. In: *ANTS 2006*. (2006) 222–237

- [4] Chen, Y.: Réduction de réseau et sécurité concrète du chiffrement complètement homomorphe. PhD thesis (2013)
- [5] Chen, Y., Nguyen, P.Q.: BKZ 2.0: Better lattice security estimates. In: ASIACRYPT 2011. (2011) 1–20
- [6] Ducas, L., Durmus, A., Lepoint, T., Lyubashevsky, V.: Lattice signatures and bimodal gaussians. In: CRYPTO 2013. (2013) 40–56
- [7] Gama, N., Howgrave-Graham, N., Koy, H., Nguyen, P.Q.: Rankin’s constant and blockwise lattice reduction. In: CRYPTO 2006. (2006) 112–130
- [8] Gama, N., Nguyen, P.Q.: Finding short lattice vectors within mordell’s inequality. In: STOC 2008. (2008) 207–216
- [9] Gama, N., Nguyen, P.Q.: Predicting lattice reduction. In: EUROCRYPT 2008. (2008) 31–51
- [10] Gama, N., Nguyen, P.Q., Regev, O.: Lattice enumeration using extreme pruning. In: EUROCRYPT 2010. (2010) 257–278
- [11] Goldstein, D., Mayer, A.: On the equidistribution of hecke points. *Forum Mathematicum* **15**(2) (2003) 165–189
- [12] Hanrot, G., Pujol, X., Stehlé, D.: Analyzing blockwise lattice algorithms using dynamical systems. In: CRYPTO 2011. (2011) 447–464
- [13] Hanrot, G., Stehlé, D.: Improved analysis of Kannan’s shortest lattice vector algorithm. In: CRYPTO 2007. (2007) 170–186
- [14] Hoffstein, J., Pipher, J., Silverman, J.H.: NTRU: A ring-based public key cryptosystem. In: ANTS 1998. (1998) 267–288
- [15] Lenstra, A.K., Lenstra, H.W., Lovász, L.: Factoring polynomials with rational coefficients. *Mathematische Annalen* **261**(4) (1982) 515–534
- [16] Massey, F.J.: The Kolmogorov-Smirnov test for goodness of fit. *Journal of the American Statistical Association* **46**(253) (1951) 68–78
- [17] Micciancio, D., Walter, M.: Practical, predictable lattice basis reduction. In: EUROCRYPT 2016. (2016) 820–849
- [18] Nguyen, P.Q., Stehlé, D.: LLL on the average. In: ANTS 2006. (2006) 238–256
- [19] Schneider, M., Buchmann, J.A.: Extended lattice reduction experiments using the BKZ algorithm. In: Sicherheit 2010. (2010) 241–252
- [20] Schnorr, C.P., Euchner, M.: Lattice basis reduction: Improved practical algorithms and solving subset sum problems. *Mathematical Programming* **66**(1-3) (1994) 181–199
- [21] Schnorr, C.P.: Lattice reduction by random sampling and birthday methods. In: STACS 2003. (2003) 145–156
- [22] Schnorr, C.: A hierarchy of polynomial time lattice basis reduction algorithms. *Theoretical Computer Science* **53**(2-3) (1987) 201–224
- [23] The FPLLL development team: `fpLLL`, a lattice reduction library. Available at <https://github.com/fplll/fplll> (2016)
- [24] The FPLLL development team: `fpYLLL`, a python interface for `fpLLL`. Available at <https://github.com/fplll/fpylll> (2016)
- [25] The FPLLL development team: `strategizer`, BKZ 2.0 strategy search. Available at <https://github.com/fplll/strategizer> (2016)

- [26] Walter, M.: BKZ simulator. Available at [http://cseweb.ucsd.edu/~miwalter/src/sim\\_bkz.sage](http://cseweb.ucsd.edu/~miwalter/src/sim_bkz.sage) (2014)
- [27] Walter, M.: Lattice point enumeration on block reduced bases. In: ICITS 2015. (2015) 269–282

## A Experimental Data

**Table 1.** Experimental Data for BKZ measure over 100-dimensional lattices

blocksize $\beta$	$e$	$s^{(h)}$	$w^{(h)}$	$w^{(t)}$	$v$	$c$
2	0.0433	0.5031	2.3466	2.1381	$0.2726 \times 10^{-2}$	$-0.0686 \times 10^{-2}$
3	0.0366	0.4441	2.0121	2.0357	$0.1947 \times 10^{-2}$	$-0.0910 \times 10^{-2}$
4	0.0344	0.4278	1.9081	1.9248	$0.1749 \times 10^{-2}$	$-0.0841 \times 10^{-2}$
5	0.0330	0.4149	1.8427	1.8722	$0.1681 \times 10^{-2}$	$-0.0820 \times 10^{-2}$
6	0.0320	0.4082	1.7951	1.8243	$0.1632 \times 10^{-2}$	$-0.0789 \times 10^{-2}$
8	0.0305	0.3939	1.7258	1.7707	$0.1581 \times 10^{-2}$	$-0.0755 \times 10^{-2}$
10	0.0295	0.3854	1.6851	1.7347	$0.1545 \times 10^{-2}$	$-0.0728 \times 10^{-2}$
12	0.0287	0.3754	1.6411	1.7165	$0.1524 \times 10^{-2}$	$-0.0707 \times 10^{-2}$
14	0.0281	0.3669	1.6027	1.7006	$0.1493 \times 10^{-2}$	$-0.0684 \times 10^{-2}$
16	0.0275	0.3844	1.7856	1.9198	$0.1477 \times 10^{-2}$	$-0.0671 \times 10^{-2}$
18	0.0271	0.4238	2.1930	2.4021	$0.1453 \times 10^{-2}$	$-0.0660 \times 10^{-2}$
20	0.0267	0.4599	2.6238	2.9502	$0.1420 \times 10^{-2}$	$-0.0642 \times 10^{-2}$
22	0.0264	0.4900	3.0578	3.5725	$0.1381 \times 10^{-2}$	$-0.0622 \times 10^{-2}$
24	0.0260	0.5165	3.4895	4.2238	$0.1351 \times 10^{-2}$	$-0.0606 \times 10^{-2}$
26	0.0255	0.5440	3.9594	4.9311	$0.1330 \times 10^{-2}$	$-0.0595 \times 10^{-2}$
28	0.0250	0.5730	4.4643	5.6665	$0.1319 \times 10^{-2}$	$-0.0590 \times 10^{-2}$
30	0.0246	0.6041	5.0257	6.4387	$0.1294 \times 10^{-2}$	$-0.0576 \times 10^{-2}$

**Table 2.** Experimental Data for BKZ 2.0 with  $C = 0.25$  measure over 180-dimensional lattices

blocksize $\beta$	$e$	$s^{(h)}$	$w^{(h)}$	$w^{(t)}$	$v$
2	0.0444	0.5212	2.4264	1.9816	$0.2749 \times 10^{-2}$
6	0.0331	0.4185	1.8899	1.9086	$0.1557 \times 10^{-2}$
10	0.0305	0.3937	1.7115	1.7218	$0.1532 \times 10^{-2}$
14	0.0284	0.3744	1.6784	1.6966	$0.1591 \times 10^{-2}$
18	0.0273	0.4161	2.1773	2.3745	$0.1431 \times 10^{-2}$
22	0.0267	0.4909	3.0054	3.5458	$0.1483 \times 10^{-2}$
26	0.0271	0.5522	4.0003	4.9496	$0.1372 \times 10^{-2}$
30	0.0272	0.6396	5.3522	6.5021	$0.1469 \times 10^{-2}$
34	0.0272	0.7223	6.7520	8.0585	$0.1258 \times 10^{-2}$
38	0.0266	0.8204	8.7515	10.0917	$0.1345 \times 10^{-2}$
42	0.0260	0.9252	10.9516	11.7763	$0.1327 \times 10^{-2}$
46	0.0252	1.0202	13.1971	14.0029	$0.1250 \times 10^{-2}$
50	0.0248	1.1003	15.2931	15.6982	$0.1044 \times 10^{-2}$
54	0.0243	1.1848	17.3093	17.8930	$0.0950 \times 10^{-2}$
58	0.0237	1.2529	19.7149	20.0544	$0.1047 \times 10^{-2}$
62	0.0231	1.3206	22.2596	22.3333	$0.1020 \times 10^{-2}$

**Table 3.** Experimental Data for BKZ 2.0 with  $C = 2.0$  measure over 180-dimensional lattices

blocksize $\beta$	$e$	$s^{(h)}$	$w^{(h)}$	$w^{(t)}$	$v$
2	0.0444	0.5212	2.4264	1.9816	$0.2749 \times 10^{-2}$
6	0.0331	0.4185	1.8899	1.9086	$0.1557 \times 10^{-2}$
10	0.0305	0.3937	1.7115	1.7218	$0.1532 \times 10^{-2}$
14	0.0284	0.3744	1.6784	1.6966	$0.1591 \times 10^{-2}$
18	0.0273	0.4161	2.1773	2.3745	$0.1431 \times 10^{-2}$
22	0.0262	0.4831	2.9479	3.5316	$0.1393 \times 10^{-2}$
26	0.0267	0.5376	3.9116	4.9197	$0.1406 \times 10^{-2}$
30	0.0268	0.6060	5.2215	6.4799	$0.1474 \times 10^{-2}$
34	0.0271	0.6519	6.0523	8.0022	$0.1397 \times 10^{-2}$
38	0.0264	0.7659	8.1996	10.1732	$0.1322 \times 10^{-2}$
42	0.0259	0.8576	10.2454	11.9750	$0.1221 \times 10^{-2}$
46	0.0255	0.9643	12.3901	13.6241	$0.1349 \times 10^{-2}$
50	0.0248	1.0478	14.5060	15.8849	$0.0978 \times 10^{-2}$
54	0.0242	1.1293	16.8939	18.0491	$0.1024 \times 10^{-2}$
58	0.0239	1.1936	19.0415	19.9118	$0.0965 \times 10^{-2}$
62	0.0232	1.2566	21.2967	22.5572	$0.0869 \times 10^{-2}$

**Table 4.** Experimental Data for BKZ 2.0 with  $C = 8.0$  measure over 180-dimensional lattices

blocksize $\beta$	$e$	$s^{(h)}$	$w^{(h)}$	$w^{(t)}$	$v$
2	0.0444	0.5212	2.4264	1.9816	$0.2749 \times 10^{-2}$
6	0.0331	0.4185	1.8899	1.9086	$0.1557 \times 10^{-2}$
10	0.0305	0.3937	1.7115	1.7218	$0.1532 \times 10^{-2}$
14	0.0284	0.3744	1.6784	1.6966	$0.1591 \times 10^{-2}$
18	0.0273	0.4161	2.1773	2.3745	$0.1431 \times 10^{-2}$
22	0.0262	0.4826	2.9618	3.5576	$0.1360 \times 10^{-2}$
26	0.0262	0.5498	3.9654	5.0129	$0.1385 \times 10^{-2}$
30	0.0268	0.5661	4.5679	6.4380	$0.1321 \times 10^{-2}$
34	0.0266	0.6486	5.9330	8.3219	$0.1416 \times 10^{-2}$
38	0.0266	0.7218	7.3683	9.7274	$0.1363 \times 10^{-2}$
42	0.0260	0.8029	9.4220	11.8752	$0.1207 \times 10^{-2}$
46	0.0253	0.9202	11.8418	13.8813	$0.1215 \times 10^{-2}$
50	0.0248	1.0134	14.0805	15.8278	$0.1001 \times 10^{-2}$
54	0.0242	1.0880	16.2848	17.9552	$0.1051 \times 10^{-2}$

**Table 5.** Simulated Data with dimension 400

blocksize $\beta$	$e$	$s^{(h)}$	$w^{(h)}$	$w^{(t)}$
6	0.0297	0.4394	1.7624	1.6903
10	0.0297	0.4394	1.7624	1.6903
14	0.0297	0.4394	1.7624	1.6903
18	0.0297	0.5280	2.5152	2.4130
22	0.0297	0.6463	3.7275	3.5771
26	0.0294	0.7625	5.1492	5.1098
30	0.0288	0.8637	6.6956	6.6455
34	0.0280	0.9477	8.2959	8.2534
38	0.0272	1.0305	10.0512	10.0095
42	0.0262	1.0999	11.8272	11.7856
46	0.0246	1.1290	13.2717	13.2449
50	0.0242	1.2054	15.3726	15.3416
54	0.0237	1.2766	17.5578	17.5152
58	0.0232	1.3418	19.7975	19.7598
62	0.0227	1.4031	22.1049	22.0706

## B Proof of Corollary 1

From Eq. (1), we have:

$$\ln(\mathbf{rhf}(\mathbf{B})) = \frac{1}{n^2} \sum_{1 \leq i \leq n-1} (n-i)r_i(\mathbf{B}). \quad (8)$$

Taking expectations, then:

$$n^2 \mathbf{E}(\ln(\mathbf{rhf}(\mathbf{B}))) = \sum_{i \leq h} (n-i)e_i^{(h)}(\beta) + \sum_{i \leq t} ie_i^{(t)}(\beta) + \sum_{h < i < n-t} (n-i)e(\beta). \quad (9)$$

Note that

$$\sum_{i \leq h} (n-i)e_i^{(h)}(\beta) + \sum_{i \leq t} ie_i^{(t)}(\beta) = \left( \sum_{i \leq t} ie_i^{(t)}(\beta) - \sum_{i \leq h} ie_i^{(h)}(\beta) \right) + n \sum_{i \leq h} e_i^{(h)}(\beta)$$

and

$$\sum_{h < i < n-t} (n-i)e(\beta) = \left( \frac{n^2}{2} - \frac{n(2h+1)}{2} \right) e(\beta) + \frac{(h-t)(h+t+1)}{2} e(\beta).$$

Since  $h$  and  $t$  are constant, the two terms  $\left( \sum_{i \leq t} ie_i^{(t)}(\beta) - \sum_{i \leq h} ie_i^{(h)}(\beta) \right)$  and  $\frac{(h-t)(h+t+1)}{2} e(\beta)$  are  $O(1)$ . A straightforward computation then leads to the conclusion.

## C Proof of Corollary 2

We compare the variances of two sides in Eq. (8), then:

$$\begin{aligned} n^4 \mathbf{Var}(\ln(\mathbf{rhf}(\mathbf{B}))) &= \sum_{i=1}^{n-1} (n-i)^2 \mathbf{Var}(r_i) + 2 \sum_{i < j} (n-i)(n-j) \mathbf{Cov}(r_i, r_j) \\ &= \sum_{i=1}^{n-1} (n-i)^2 \mathbf{Var}(r_i) + 2 \sum_{i=1}^{n-2} (n-i)(n-i-1) \mathbf{Cov}(r_i, r_{i+1}). \end{aligned} \quad (10)$$

Splitting the sum  $\sum_{i=1}^{n-1} (n-i)^2 \mathbf{Var}(r_i)$  into three parts, we have:

$$\sum_{i=1}^{n-1} (n-i)^2 \mathbf{Var}(r_i) = \sum_{i \leq h} (n-i)^2 \mathbf{Var}(r_i) + \sum_{i \geq n-t} (n-i)^2 \mathbf{Var}(r_i) + \sum_{h < i < n-t} (n-i)^2 \mathbf{Var}(r_i). \quad (11)$$

Both  $h$  and  $t$  are constant and the variances  $\mathbf{Var}(r_i)$ 's with  $i \leq h$  or  $i \geq n-t$  are also constant. Thus the two first sums are  $O(n^2)$ . Also, the difference  $\sum_{i=1}^{n-1} (n-i)^2 \mathbf{Var}(r_i) - \sum_{h < i < n-t} (n-i)^2 \mathbf{Var}(r_i)$  is  $O(n^2)$ , then:

$$\begin{aligned} \sum_{h < i < n-t} (n-i)^2 \mathbf{Var}(r_i) &= \sum_{i=1}^{n-1} (n-i)^2 \mathbf{Var}(r_i) + O(n^2) \\ &= \frac{n(n-1)(2n-1)}{6} \mathbf{Var}(r) + O(n^2) \\ &= \frac{n^3}{3} v(\beta) + O(n^2). \end{aligned} \quad (12)$$

The sum  $\sum_{i=1}^{n-2} (n-i)(n-i-1)\mathbf{Cov}(r_i, r_{i+1})$  can be split into three parts:

$$\sum_{i \leq h} (n-i)(n-i-1)\mathbf{Cov}(r_i, r_{i+1}) + \sum_{i \geq n-t} (n-i)(n-i-1)\mathbf{Cov}(r_i, r_{i+1}) + \sum_{h < i < n-t} (n-i)(n-i-1)c(\beta). \quad (13)$$

Since all  $\mathbf{Cov}(r_i, r_{i+1})$ 's inside the head and tail are of size  $O(1)$ , the first two sums are  $O(n^2)$ . The difference  $\sum_{i=1}^{n-2} (n-i)(n-i-1)c(\beta) - \sum_{h < i < n-t} (n-i)(n-i-1)c(\beta)$  is also  $O(n^2)$ , then:

$$\begin{aligned} & \sum_{h < i < n-t} (n-i)(n-i-1)\mathbf{Cov}(r_i, r_{i+1}) \\ &= \sum_{i=1}^{n-2} (n-i)(n-i-1)c(\beta) + O(n^2) \\ &= \left( \frac{(n-2)(n-1)(2n-3)}{6} + \frac{(n-2)(n-1)}{2} \right) \cdot c(\beta) + O(n^2) \\ &= \frac{n^3}{3}c(\beta) + O(n^2). \end{aligned} \quad (14)$$

Combining Eq. (10), (12) and (14), we complete the proof.

## D Proof of Corollary 3

Let  $n' = \lfloor \frac{n}{2} \rfloor$ . A routine computation leads to that:

$$\mathbf{h}\mathbf{v}(\beta, n) = \left(1 - \frac{n'}{n}\right) \sum_{i=1}^{n'} ir_i + \frac{n'}{n} \sum_{i=n'+1}^{n-1} (n-i)r_i. \quad (15)$$

We compare the expectations of two sides in Eq. (15), then:

$$\begin{aligned} \mathbf{E}(\mathbf{h}\mathbf{v}(\beta, n)) &= \left(1 - \frac{n'}{n}\right) \left( \sum_{i \leq h} ie_i^{(h)}(\beta) \right) + \frac{n'}{n} \left( \sum_{i \leq t} ie_i^{(t)}(\beta) \right) \\ &+ \left( \frac{n'(n-n')}{2} - \frac{(n-n')h(h+1) + n't(t+1)}{2n} \right) e(\beta). \end{aligned} \quad (16)$$

Since  $h$  and  $t$  are constant, the two sums  $\sum_{i \leq h} ie_i^{(h)}(\beta)$  and  $\sum_{i \leq t} ie_i^{(t)}(\beta)$  are  $O(1)$ . Note that  $n' = \frac{n}{2} + O(1)$  and  $n'(n-n') = \frac{n^2}{4} - \frac{1}{2}\{\frac{n}{2}\}$ , which proves Eq. (4).

We compare the variances of two sides in Eq. (15), then:

$$\begin{aligned}
\mathbf{Var}(\mathbf{hv}(\beta, n)) &= \left(1 - \frac{n'}{n}\right)^2 \left(\sum_{i \leq h} i^2 v_i^{(h)}(\beta)\right) + \left(\frac{n'}{n}\right)^2 \left(\sum_{i \leq t} i^2 v_i^{(t)}(\beta)\right) \\
&+ \left(\frac{n'(n-n')(2n'(n-n')+1)}{6n} - \left(1 - \frac{n'}{n}\right)^2 \sum_{i \leq h} i^2 - \left(\frac{n'}{n}\right)^2 \sum_{i \leq t} i^2\right) v(\beta) \\
&+ 2 \left(1 - \frac{n'}{n}\right)^2 \sum_{i < n'} i(i+1) \mathbf{Cov}(r_i, r_{i+1}) \\
&+ 2 \left(\frac{n'}{n}\right)^2 \sum_{i < n-n'-1} i(i+1) \mathbf{Cov}(r_{n-i}, r_{n-i-1}) \\
&+ 2 \left(1 - \frac{n'}{n}\right) \left(\frac{n'}{n}\right) n'(n-n'-1) \mathbf{Cov}(r_{n'}, r_{n'+1})
\end{aligned} \tag{17}$$

We substitute all  $\mathbf{Cov}(r_i, r_{i+1})$ 's by  $c(\beta)$ , which only leads to a  $O(1)$  difference. Exploiting the identity that  $\sum_{i=1}^n i(i+1) = \frac{n(n+1)(n+2)}{3}$ , we know the sum of a batch of local covariances in Eq. (17) equals  $\frac{2n'(n-n')(n'(n-n')-1)}{3n} c(\beta) + O(1)$ . Thus we have:

$$\mathbf{Var}(\mathbf{hv}(\beta, n)) = \frac{n'(n-n')(2n'(n-n')+1)}{6n} v(\beta) + \frac{2n'(n-n')(n'(n-n')-1)}{3n} c(\beta) + O(1), \tag{18}$$

which implies Eq. (5).